UC Davis

UC Davis Previously Published Works

Title

Formation of liquid–liquid slug flow in a microfluidic T-junction: Effects of fluid properties and leakage flow

Permalink

https://escholarship.org/uc/item/0p545152

Journal

AIChE Journal, 64(1)

ISSN

0001-1541

Authors

Yao, Chaoqun
Liu, Yanyan
Xu, Chao
et al.

Publication Date

2018

DOI

10.1002/aic.15889

Peer reviewed

eScholarship.org Powered by the California Digital Library
University of California

Molecular Simulation Study of Aluminum – Noble Gas Interfacial Thermal Accommodation Coefficients

Haoyan Sha [1], Gulcin Tetiker [2], Peter Woytowitz [3], Roland Faller [1 1]

[1] Department of Chemical Engineering, University of California-Davis, Davis, CA, 95616

[2] Lam Research Corporation, Fremont, CA, 94538

[3] Arevo Labs Inc., Santa Clara, CA 95054

ABSTRACT

Thermal accommodation coefficients (TAC) between aluminum and noble gases were studied with molecular dynamics (MD) simulations. Gases interacting with aluminum substrates were modeled by MD with gas velocities sampled from the Maxwell – Boltzmann distribution to give accumulated TAC results. Different implementations of the equation to calculate the TAC, which differ in the amount of information gleaned from MD and the corresponding simulation results, were carefully discussed. The best formula for molecular dynamics modeling in finite simulation time was determined. Additionally, the influence of the combining rules applied on aluminum – noble gas interatomic potential was characterized with the well-known Lennard – Jones 12 – 6 potential combined with Lorentz – Berthelot and Fender – Halsey mixing rules. The results were compared with experimental values and previous analytical model. TACs simulated with Fender – Halsey rules present excellent agreement with the experimental values. Detailed TAC distributions and accumulated TAC convergence are also included.

1 Corresponding author.

Email: rfaller@ucdavis.edu

Topical Heading: Thermodynamics and Molecular-Scale Phenomena

Keywords: thermal accommodation coefficient, molecular dynamics, heat transfer

INTRODUCTION

Interfacial heat transfer is an important topic in a wide variety of science and engineering applications, such as semiconductor physics, heat exchange in the oil & gas industry, and the cooling of microelectronic devices [1-5]. Especially in the semiconductor industry, many of the etching and atomic deposition processes are very temperature sensitive. To accurately model the operation temperature, good heat transfer estimation methods are required.

The thermal accommodation coefficient (TAC) is commonly utilized to evaluate the heat transfer efficiency [6]. It was first proposed a century ago and later was developed as a constant to represent the extent of energy transfer of gas molecules striking a solid surface [7]. Generally, the TAC expresses the ratio of actual energy change versus the maximal theoretical energy difference between the two phases. Its value normally ranges from 0, indicating no heat exchange at all, to 1, which means full heat transfer.

Besides the experimental efforts in calculating TAC [8-11], theoretical methods have been developed to study the heat transfer process and derive the TAC values. Fan and Manson proposed a classical mechanical theory based on an analytical model for the accommodation of rare gases interacting with a tungsten surface [12]. Giri and Hopkins developed a model with the diffuse mismatch theory to understand gold – gas thermal accommodation and conductance. Their results were compared with the TAC result derived from Non Equilibrium Molecular Dynamics (NEMD) simulations [13].

With the technology development stepping into micro and nano scales, a global description of heat transfer becomes insufficient. Instead, a more detailed understanding of the heat exchange process at the atomic level is crucial to further research and development. Several molecular dynamics (MD)

studies have been performed to reproduce the interfacial physical thermal processes. Daun et al. studied the TACs at interfaces between noble gases and nickel particles and graphite in laser-induced incandescence processes [14,15]. Sipkens et al. performed in situ nanoparticle size measurements of gas-borne silicon nanoparticles by time-resolved laser-induced incandescence [16]. Liang and Keblinski investigated the TACs of gold and monoatomic and diatomic gases [17]. Westergren and Gronbeck explored the noble gas and Pd cluster interaction [18]. On the methodological side, Liang et al. compared thermal conductance results from equilibrium and non-equilibrium molecular dynamics simulations, and showed that both methods provide similar results [19].

To our best knowledge, the TAC at the aluminum – noble gas interface, which has important applications in atomic deposition in semiconductor industry, has not been studied in detail by molecular modeling. Moreover, from a methodological standpoint, different implementation of the equation to derive TAC with different statistical thermodynamics expressions have not been well analyzed and validated for molecular dynamics in finite simulation time.

In the present study, we apply molecular dynamics to model the noble gas – aluminum interfacial heat transfer processes. Three different ways to implement the equation to derive the TAC were tested and the corresponding TAC results analyzed and discussed. The best TAC formula for MD method was determined. The influence of the solid – gas interatomic potential on the TAC was also characterized. The TAC was calculated with a few potentials including the empirical Lennard – Jones potentials combined by both Lorentz – Berthelot and Fender – Halsey mixing rules. The final TAC values were then compared with previous experimental results and present excellent agreement.

MODEL & METHOD

Molecular dynamics (MD) simulations were carried out with the LAMMPS code [20] to simulate the processes of noble gas atoms interacting with aluminum substrate. The initial simulation temperatures of

the solid Al and noble gases were set as 675 K and 300 K, respectively, which correspond to the practical chamber operating temperatures in the semiconductor industry. The velocity-Verlet algorithm [21] was used for the MD time integration with a 1 fs time step. The aluminum substrate model was built with 2000 Al atoms in a face center cubic structure with the size of 40.5 Å * 40.5 Å * 20.25 Å in x, y, z directions respectively. Periodic boundary conditions were applied to present the bulk surface properties of aluminum. The solid substrate was heated up to 675 K in the NVT ensemble using a Nosé–Hoover thermostat [22,23]. The Al – Al interaction was described with the Aluminum EAM potential with a 10 Å cutoff [24]:

$$E_i = F_\alpha\left(\sum_{i\neq j}\rho_\beta(r_{ij})\right) + \frac{1}{2}\sum_{i\neq j}\phi_{\alpha\beta}(r_{ij})$$

where F is an embedding function that represents the required energy to place atom i of type α in the electron cloud, r_{ij} is the distance between atoms i and j, ρ_β is the contribution to the electron charge density from atom j, of type b at the location of atom i, $\phi_{\alpha\beta}$ is a pairwise potential function.

After the Al substrate was at the target temperature, the thermostat was turned off. A single gas atom was introduced into the simulation box 10 Å above the Al substrate just outside the interaction cutoff. The velocity of the introduced gas atom was sampled from the Maxwell-Boltzmann distribution:

$$f(v) = \sqrt{\left(\frac{m}{2\pi kT}\right)^3}\, 4\pi v^2 e^{-\frac{mv^2}{2kT}}$$

where f is the distribution probability, v is the velocity, m is the mass, k is the Boltzmann constant, and T is the temperature. No positive *z* velocity was allowed to ensure that the gas atom moves towards the

Al surface. The gas velocity distributions from the MD sampling were compared with the theoretical Maxwell – Boltzmann distribution in FIG 1 and showed good agreements.

The noble gas – aluminum interactions were described with a Lennard – Jones potential:

$$V = 4\varepsilon\left[\left(\frac{\sigma}{r}\right)^{12} - \left(\frac{\sigma}{r}\right)^{6}\right]$$

σ is the cutoff distance, ε is the potential energy well depth.

The commonly used Lorentz – Berthelot (L-B) mixing rules as well as the Fender – Halsey (F-H) combining rules with the following formulas were applied to get the pair potentials between aluminum and noble gases. The two types of combining rules are distinguished by how the interatomic energy term of the L-J potential between atoms of different types is determined:

Lorentz – Berthelot:

$$\sigma_{ij} = \frac{\sigma_{ii} + \sigma_{ij}}{2}, \quad \varepsilon_{ij} = \sqrt{\varepsilon_{ii}\varepsilon_{jj}}$$

Fender – Halsey:

$$\sigma_{ij} = \frac{\sigma_{ii} + \sigma_{ij}}{2}, \quad \varepsilon_{ij} = \frac{2\varepsilon_{ii}\varepsilon_{jj}}{\varepsilon_{ii} + \varepsilon_{jj}}$$

As is shown explicitly by Daun et al. by comparing the Lorentz – Berthelot (L-B) rules mixed Lennard – Jones potential with the density functional theory (DFT) fitted potential [15,25], the widely used L-B mixing rule overestimates the potential energy strength, especially for the short-range repulsion. Therefore, a relatively softer energy combining method involved in the F-H mixing rules were tested as well. Both rules obtain the same interaction distance and base on a geometric mixing of the interaction

energies such that there are little fundamental arguments in favor of one over the other. The F-H mixing rules correct the potentials in the same direction as the DFT, which soften the potential energy strength. Theoretically, the F-H rules deliver more accurate potential approximation when the atomic radii and diamagnetic coefficients of the two materials are close. The detailed Al – noble gas interatomic potential parameters of the selected potential models are listed in TABLE I.

To calculate the energy transfer during the gas – solid interaction, the NVE ensemble was applied. The kinetic energy of the gas atom was recorded before entering the cutoff distance with the Al surface and again once it leaves. No re-enter of the gas atom to the interaction zone was allowed.

A single gas atom interacting with the Al surface was utilized here. At a gas temperature of 300 K and below 1.5 Pa, only less than 2% gas – gas collisions are expected [18]. The low gas – gas collision possibility suggests that the collision is negligible. This complete velocity sampling and MD simulation processes were then repeated for many times to calculate TAC values.

RESULTS & DISCUSSION

Three formulas of the equation to derive TAC are introduced below, which all represent the ratio of the energy change of the gas atom in the heat transfer process over the theoretical maximum, but with different statistical thermodynamics expressions

$$\alpha = \frac{\langle E_0 - E_i \rangle}{2k_B(T_s - T_g)} \qquad \text{Formula 1}$$

$$\alpha = \frac{\langle E_0 - 2k_B T_g \rangle}{2k_B(T_s - T_g)} \qquad \text{Formula 2}$$

$$\alpha = \left\langle \frac{E_0 - E_i}{2k_B T_s - E_i} \right\rangle$$ Formula 3

where E_0 is the gas kinetic energy outlet the cutoff distance, E_i is the inlet gas kinetic energy, k_B is the Boltzmann constant, T_s is the initial aluminum surface temperature, T_g is the target initial gas phase temperature.

Formula 1 is the most used formula in analytical methods and was previously applied in MD simulations to calculate TAC [14,15]. The numerator shows the average of the gas atom energy difference in each individual simulation over many repeats, while the denominator uses the global temperatures of the solid aluminum and the gas phase to express the maximum heat flux that can be transferred. However, the accuracy highly depends on how well the model represents ergodicity, especially when the numerator depends on the simulations and the denominator does assume perfect convergence. To test the accuracy of the formula in the MD simulations, which have finite simulation time, two other formulas that maximize information gleaned from the individual simulations (Formula 3) and which maximize information from assumed convergence (Formula 2) were tested and applied in the TAC calculations.

Particularly, in formula 2, the individual initial gas velocity term in the numerator is replaced with the global gas temperature, as the full set of velocities of the gas atoms match the Maxwell – Boltzmann distribution at the assigned temperature. The denominator is kept the same as in formula 1. In formula 3, compared to formula 1, the actual energy transferred from Al to the gas is the same, but the gas phase heat flux term in the denominator was replaced with the individual initial energy of the gas atom. E_0, which represents the outlet energy of the gas after interacting with the hot Al substrate in each

simulation, is not replaceable with a global representation. Also, the statistical averaging is in formula 3 after the calculation of the complete individual TAC. In formulas 1 and 2 the numerator and denominator are pre-averaged leading to different sampling.

MD simulations were performed with the interatomic potentials listed in the method section. For the helium – aluminum case, in most instances, the helium atom just hit the Al substrate once and leaves the interaction zone, as shown in FIG. 2, in a close to elastic collision. The low atomic weight helium atom interacts only weakly with aluminum. Argon atoms with stronger pair potential with the Al substrate are more likely to hop a few times on the Al surface. The number of hops varies depending on the initial gas velocity and the inlet angle towards the solid surface. The different sets of potential parameters only affected the strength of noble gases interacting with the Al solid surface, while the dynamic behavior of the gas atoms was not changed.

The accumulated TACs were calculated with the 3 formulas of the TAC equation and the values were listed in TABLE II. For the helium – aluminum case, each MD simulation was run for 100 ps, which is long enough for the atom to interact with the solid and leave the cutoff distance. The classical Lorentz – Berthelot (L-B) mixing rules gave TAC values of -1.5189, 1.7078, and 0.7195, while the Fender – Halsey (F-H) mixing rules leaded to -0.8284, 2.4074, and 0.3653, which are corresponding to Formulas 1 to 3 respectively. With both combining rules, Formula 1 gives negative values and Formula 2 provides positive ones but much larger than unity, which represent either an inversed heat flow from low temperature gas to hot solid or an unphysically large heat flux over the thermodynamic maxima set by the 2nd law. Only formula 3 that includes the most individual representations delivers TACs between theoretical thresholds 0 and 1. For the argon – aluminum case, the L-B combining rules give values of 1.3974, 1.0088, and 1.0182, while F-H presents TACs of 1.1993, 0.8070, and 0.8614, corresponding to TAC equation formula 1

– 3. The TAC uncertainties are estimated by the data standard error. In this case, Formula 1 still gives widely unrealistic results, while the other two are similar at 1 and 0.86, respectively for LB and FH.

For Table II, the TACs derived with the individually calculated energy flux terms and the globally assumed ones present a large difference. As we can see from both noble gas cases, Formula 1 that mixes global and individual representations gives the most unrealistic TACs. Formula 2 which maximizes global assumed converged terms gives unphysical TACs for the helium – aluminum pair, but can somewhat describe the argon case. The TAC values from each individual MD simulation were plotted versus the initial gas velocity with the data collected with the F-H rules, as shown in FIG. 3. The accumulated TAC values from formula 1 and 2, which have the same and fixed representations in the denominators, have a large contribution from simulations with high initial velocities. The difference in numerator description leads to either larger than 1 or negative accumulated TAC values. For formula 3, the denominator is specified towards each individual case, and so the largest contribution comes from the most probable velocity range according to the M-B velocity distribution shown in FIG. 1. It makes sense that the area around the most probable velocity contributes most to the TAC.

Note that in FIG 3a we see at high gas velocities (above 700 m/s) a larger number of individual negatives TAC which indicates that for faster (hotter) gas molecules the likelihood of a reverse heat transfer increases.

It appears that the larger atomic mass of argon can significantly reduce the uncertainty of energy transfer fluctuation, as Ar has a relatively narrow velocity range in the M-B distribution; while the lightweight helium energy transfer process is highly inlet velocity dependent. Formula 2 only works on large atomic mass atoms and there it likely overestimates the TAC with perfect transfer. Comparing to the first two, Formula 3, which includes the most individual case details, consistently provides physical TAC results, so that we suggest that it is the best formula to be utilized in MD simulations to derive TACs.

To compare the mixing rules impact on the TAC, the interatomic potentials of noble gases with the aluminum substrate are plotted in FIG. 4. The F-H mixing rules provide much softer potentials than the L-B rules, in which the gas atom relatively weakly interacts with the aluminum substrate and can get closer to the solid surface. For helium, with both combining rules, the gas atom only hits the aluminum surface once in most cases. For argon, which has a stronger interaction with the substrate, LB presents shorter interaction times and less hops on the Al surface.

TAC results from both combining rules calculated by Formula 3 are also compared with published experimental data to evaluate the TACs and validate our MD simulation model (TABLE II). For argon – aluminum, the experimental TAC was reported as 0.86 [29], or 0.91 to 0.96 [28] for a gas temperature of 300 K. The differences in the experimental values were due to the surface condition and the pre-measurement treatment. The aluminum surface condition could significantly affect the energy transfer rate between the solid and the light gas atoms [31]. In comparison to the experimental value, our MD simulations with the F-H rule obtain a TAC of 0.86, which matches the value reported in ref [29] and reasonably agrees with the other. The L-B value results to a TAC of 1.02, which is slightly above unity and essentially would mean perfect heat exchange. For helium – aluminum, the experimental TAC of a machined Al surface is 0.47 and the cleaner Al surface with a plasma treatment is 0.38 [28,29]. Our MD simulation yields for the F-H model a TAC value of 0.36 and the L-B value is around 0.72. In both cases, the Lorentz – Berthelot mixing rules result in too large heat transfer and overestimate the TAC values, while the Fender-Halsey rules can excellently reproduce the experimental results. It should be noted that the experimental determination of TAC has its own uncertainties depending on the particular materials and experimental conditions. Here the values are just used to confirm the estimated results of our MD model. Also comparing to the previous analytical model, [30] our MD method provides TACs in better agreement with experimental data and more atomistic physics information of the gas – solid heat transfer process.

FIG. 5 shows scatterplots with TAC values from each individual simulation and the corresponding histograms in, both, the He – Al and Ar – Al cases, to express the TAC distributions. The TAC data points were simulated with the Fender – Halsey combining rules and the TAC values were calculated with formula 3. Note that this is different from FIG. 3 where the TAC values are ordered by gas velocity whereas they appear in FIG. 5 in the random sampling order of appearance.

We see that in individual simulations the TAC values locate on both the positive and negative axis, but most locate near the theoretical threshold range of 0 to 1. We have to keep in mind that the gas velocities were sampled from the Maxwell – Boltzmann (M-B) distribution, which leads to a rather wide velocity range. The histograms also show that the TAC distributions reflect the M-B distribution trends. When a gas with a high initial velocity is introduced, there is a high chance that the collision energy transfers from the gas to solid and makes the TAC negative. Additionally, the instantaneous local aluminum temperature is another factor that affects the collision process and the heat and momentum transfer. So, in an individual collision, the heat transfer can happen in either direction, but statistically the accumulated data is kept positive. In comparison, helium shows a wider distribution than argon. Because of the light atomic weight of helium leading to a higher velocity at the same temperature, many microscopic factors can affect the heat and momentum transfer process, such as the gas incident angle, gas initial velocity, Al local temperature, etc. On the other side, the larger and heavier argon atom's dynamic behavior is less affected by these factors. This also explains the larger uncertainties in the accumulated TAC values for He. To statistically validate the present study, the convergence of TAC with the number of individual simulation/sampling was studied towards the data sets with F-H mixing rules towards all three selected TAC formulas (shown in FIG. 6). The gas velocities were randomly sampled from M-B distribution at 300K. It can be found that for both Ar and He, the accumulated TAC values converge quite fast and become stable with about 2000 simulations. The TAC convergence data collected

with L-B mixing rules is included in the supplementary materials and also presents good convergence, which has very similar trends as F-H.

As a cutoff value is often used in theoretical methods to improve computation efficiency and convenience, we tested how the convergence of the accumulated TAC varies with the TAC cutoff value (FIG. 7). The positive limit is the same as the cutoff value on the x-axis and the negative limit equals to negative cutoff value plus one, since the theoretical TAC locates between 0 and 1. By increasing the TAC cutoff value, the accumulated TACs vary widely and get close to convergence for a cutoff larger than 15. Though the theoretical TAC value is between 0 and 1, the accumulation of TAC should take the large data points into consideration to ensure correct statistics. To ensure the quality, all presented TAC values above were calculated with a cutoff of 50.

To further validate the present TAC model, we applied MD simulations on interaction of neon and aluminum at the same conditions as He and Ar, which has no present experimental data in literature, to check the consistency. The estimated TAC values of Ne – Al derived with Formula 3 with F-H and L-B mixing rules were 0.565 and 0.910 respectively. These TAC values present great consistency with the He and Ar data. The corresponding Ne – Al TAC distribution data and mapping can be found in the supplementary document.

CONCLUSION

In the present work, the physical process of an aluminum substrate being cooled with noble gases (helium, argon) was simulated with molecular dynamics. Single gas atoms interacting with aluminum substrates were modeled multiple times to derive accumulated thermal accommodation coefficient (TAC). The methodology in deriving the TAC with MD simulations was analyzed in detail. Three formulas for TAC calculation, which involved different representations of the energy flux terms in the equation, were carefully tested and analyzed. The best formula for finite time simulations was

determined to be the one with the most individual simulation data. Different combining rules in mixing the empirical interatomic Lennard – Jones potential were utilized in the simulations to test the corresponding influence on TAC calculation. The data was compared to experimental values and previous analytical model data. The MD TACs simulated with the Fender – Halsey mixing rules present excellent agreement with the experimental data collected at different conditions. Comparing to the analytical model, the present method not only shows better agreement with the experiments, but also provides a detailed molecular-level picture of the gas – solid heat transfer process from the simulations. The TAC statistical distribution and the convergence of accumulated TAC value with number of simulation and TAC cutoff are also discussed. The present MD method converges in less than 2000 times sampling.

The current study utilized the NVE MD method, whereas in other studies NVT MD, Monte Carlo, and other methods might be applied. The evaluated best formula for TAC determination and the associated soft F-H mixing rules are expected to be valid in other systems and methods as well, with considering particular dominate factors and necessary modifications in each circumstance.

ACKNOWLEDGEMENT

We acknowledge many helpful discussions with Jack Mclnerney, and Seshu Nimmala from Lam Research Corporation. The research was financially supported by Lam Research Foundation/Silicon Valley Community Foundation.

REFERENCE

1. Hu L, Desai T, Keblinski P. Determination of interfacial thermal resistance at the nanoscale. *Physical Review B*. 05/10/ 2011;83(19):195423.

2. Ungerer P, Tavitian B, Boutin A. *Applications of molecular simulation in the oil and gas industry : Monte Carlo methods*. Paris: Technip; 2005.

3. Pierret RF. *Semiconductor device fundamentals*. Beijing: Dian zi gong ye chu ban she; 2004.

4. Goodman FO. Thermal accommodation coefficients. *The Journal of Physical Chemistry*. 1980;84(12):1431-1445.

5. Goodman FO, Wachman HY. Formula for thermal accommodation coefficients. *The Journal of Chemical Physics*. 1967;46(6):2376-2386.

6. Saxena SC, Afshar R. Thermal accommodation coefficient of gases on controlled solid surfaces: Argon-tungsten system. *International Journal of Thermophysics*. 1985// 1985;6(2):143-163.

7. Song S, Yovanovich M. Correlation of thermal accommodation coefficient for engineering surfaces. *ASME HTD*. 1987;69:107-116.

8. Yamaguchi H, Imai T, Iwai T, Kondo A, Matsuda Y, Niimi T. Measurement of thermal accommodation coefficients using a simplified system in a concentric sphere shells configuration. *Journal of Vacuum Science & Technology A*. 2014;32(6):061602.

9. Winkler P, Vrtala A, Rudolf R, et al. Condensation of water vapor: Experimental determination of mass and thermal accommodation coefficients. *Journal of Geophysical Research: Atmospheres*. 2006;111(D19).

10. Wachman HY. The thermal accommodation coefficient: a critical survey. *ARS Journal*. 1962;32(1):2-12.

11. Leroy O, Perrin J, Jolly J, Péalat M, Lefebvre M. Thermal accommodation of a gas on a surface and heat transfer in CVD and PECVD experiments. *Journal of Physics D: Applied Physics*. 1997;30(4):499.

12. Fan G, Manson JR. Calculations of the energy accommodation coefficient for gas–surface interactions. *Chemical Physics*. 5/12/ 2010;370(1–3):175-179.

13. Giri A, Hopkins PE. Analytical model for thermal boundary conductance and equilibrium thermal accommodation coefficient at solid/gas interfaces. *The Journal of Chemical Physics*. 2016;144(8):084705.

14. Daun KJ, Smallwood GJ, Liu F. Molecular dynamics simulations of translational thermal accommodation coefficients for time-resolved LII. *Applied Physics B*. 2009// 2009;94(1):39-49.

15. Daun KJ, Titantah JT, Karttunen M. Molecular dynamics simulation of thermal accommodation coefficients for laser-induced incandescence sizing of nickel particles. *Applied Physics B*. 2012// 2012;107(1):221-228.

16. Sipkens TA, Mansmann R, Daun KJ, et al. In situ nanoparticle size measurements of gas-borne silicon nanoparticles by time-resolved laser-induced incandescence. *Applied Physics B*. 2014// 2014;116(3):623-636.

17. Liang Z, Keblinski P. Parametric studies of the thermal and momentum accommodation of monoatomic and diatomic gases on solid surfaces. *International Journal of Heat and Mass Transfer*. 11// 2014;78:161-169.

18. Westergren J, Grönbeck H, Kim S-G, Tománek D. Noble gas temperature control of metal clusters: A molecular dynamics study. *The Journal of Chemical Physics*. 1997;107(8):3071-3079.

19. Liang Z, Evans W, Keblinski P. Equilibrium and nonequilibrium molecular dynamics simulations of thermal conductance at solid-gas interfaces. *Physical Review E*. 02/15/ 2013;87(2):022119.

20. Plimpton S. Fast Parallel Algorithms for Short-Range Molecular Dynamics. *Journal of Computational Physics*. 1995/03/01 1995;117(1):1-19.

21. Swope WC, Andersen HC, Berens PH, Wilson KR. A computer simulation method for the calculation of equilibrium constants for the formation of physical clusters of molecules: Application to small water clusters. *The Journal of Chemical Physics*. 1982/01/01 1982;76(1):637-649.

22. Hoover WG. Canonical dynamics: Equilibrium phase-space distributions. *Physical Review A*. 03/01/ 1985;31(3):1695-1697.

23. Nosé S. A unified formulation of the constant temperature molecular dynamics methods. *The Journal of Chemical Physics*. 1984;81(1):511-519.

24. Zope RR, Mishin Y. Interatomic potentials for atomistic simulations of the Ti-Al system. *Physical Review B*. 07/14/ 2003;68(2):024102.

25. Daun K, Sipkens T, Titantah J, Karttunen M. Thermal accommodation coefficients for laser-induced incandescence sizing of metal nanoparticles in monatomic gases. *Applied Physics B*. 2013;112(3):409-420.

26. Puri P, Yang V. Effect of Particle Size on Melting of Aluminum at Nano Scales. *The Journal of Physical Chemistry C*. 2007/08/01 2007;111(32):11776-11783.

27. Watts RO, McGee IJ. *Liquid State CHemical Physics*. New York: Wiley; 1976.

28. Trott WM, Castañeda JN, Torczynski JR, Gallis MA, Rader DJ. An experimental assembly for precise measurement of thermal accommodation coefficients. *Review of Scientific Instruments*. 2011;82(3):035120.

29. Trott WM, Rader DJ, Castañeda JN, Torczynski JR, Gallis MA. Measurement of Gas-Surface Accommodation. *AIP Conference Proceedings*. 2008;1084(1):621-628.

30. Selden N, Gimelshein N, Gimelshein S, Ketsdever A. Analysis of accommodation coefficients of noble gases on aluminum surface with an experimental/computational method. *Physics of Fluids*. 2009;21(7):073101.

31. Liang Z, Evans W, Desai T, Keblinski P. Improvement of heat transfer efficiency at solid-gas interfaces by self-assembled monolayers. *Applied Physics Letters*. 2013;102(6):061907.

List of Figure Captions:

FIG. 1. Gas velocity probability density distribution at 300K: (a) Ar; (b) He

FIG. 2. Gas atom interacts with aluminum substrate: inlet – contact – outlet

FIG. 3. Thermal accommodation coefficient vs. gas initial velocity under F-H rules: (a) Ar; (b) He

FIG. 4. Potential energy plot of noble gases interacting with aluminum substrate: (a) He – Al; (b) Ar – Al (Here the potential energy is divided by the Boltzmann constant)

FIG. 5. Thermal accommodation coefficient distribution: (a) Ar – Al TAC vs simulation count scatterplot; (b) He – Al TAC vs simulation count scatterplot; (c) Ar – Al TAC histogram; (d) He – Al TAC histogram

FIG. 6. Convergence of TAC with the number of individual simulation: (a) Ar – Al; (b) He – Al

FIG. 7. Accumulated TAC varies with the selected TAC range: (a) He – Al, (b) Ar – Al

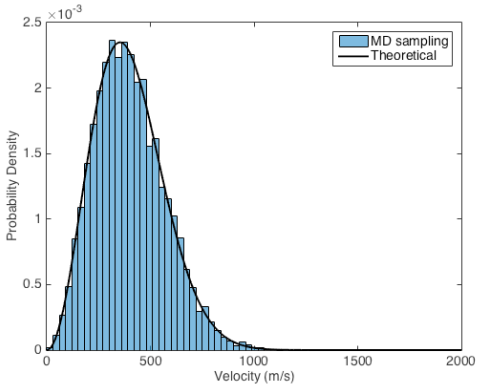

(a)

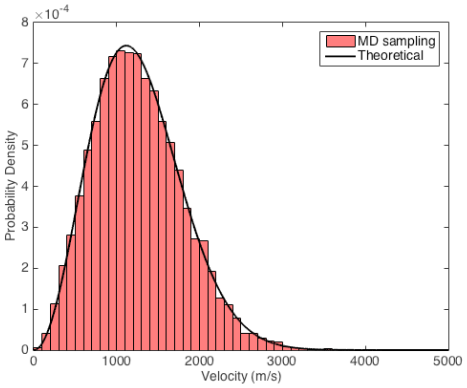

(b)

FIG. 1. Gas velocity probability density distribution at 300K: (a) Ar; (b) He

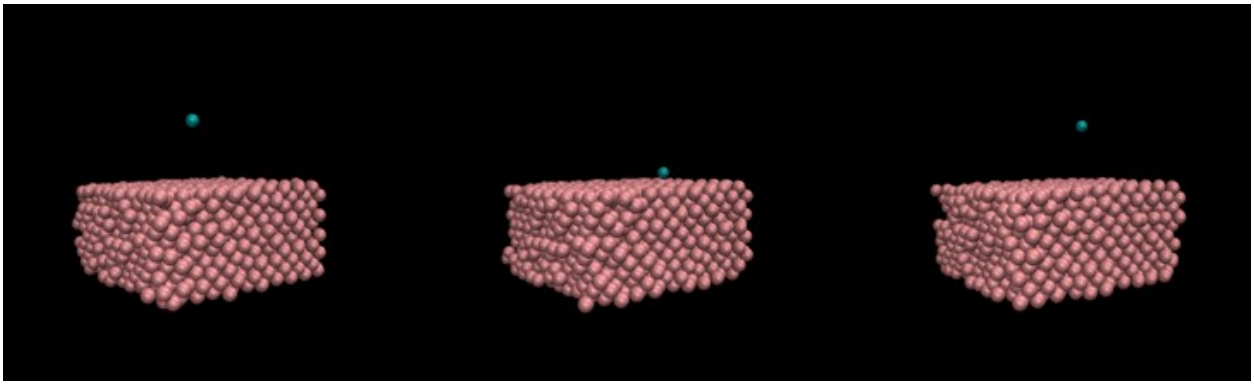

FIG. 2. Gas atom interacts with aluminum substrate: inlet – contact – outlet

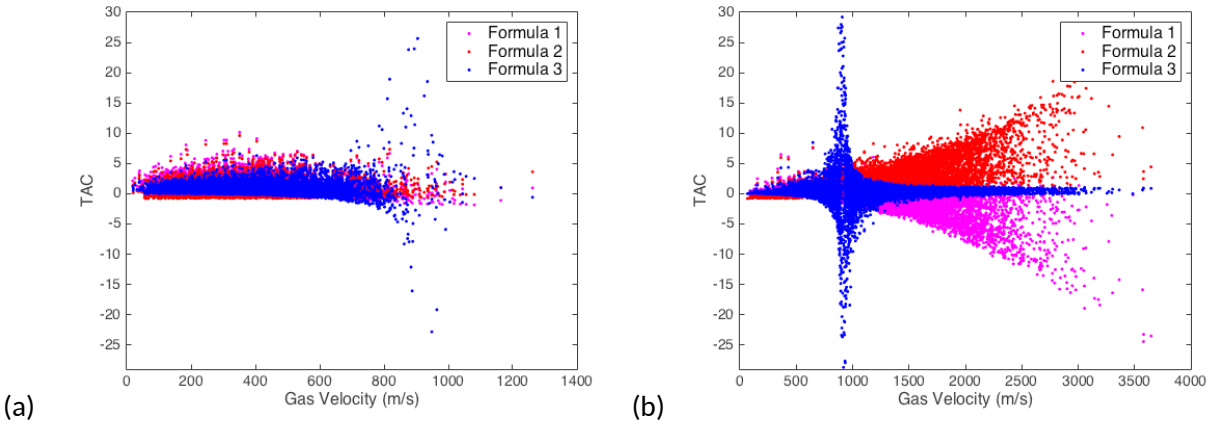

FIG. 3. Thermal accommodation coefficient vs. gas initial velocity under F-H rules: (a) Ar; (b) He

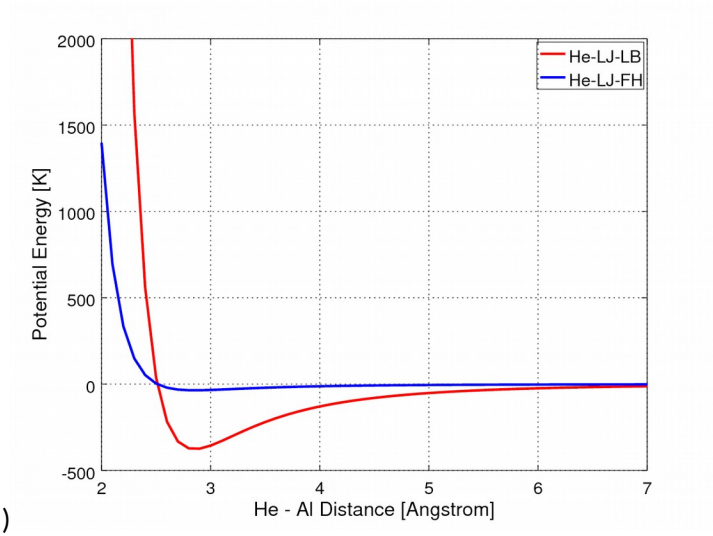

(a)

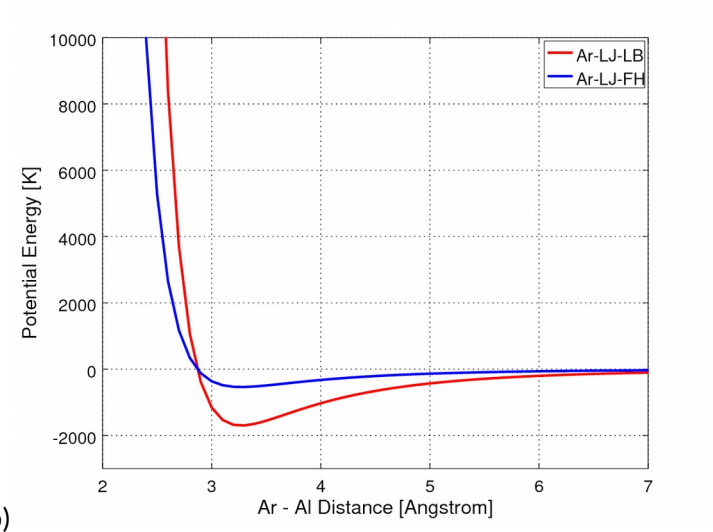

(b)

FIG. 4. Potential energy plot of noble gases interacting with aluminum substrate: (a) He – Al; (b) Ar – Al

(Here the potential energy is divided by the Boltzmann constant)

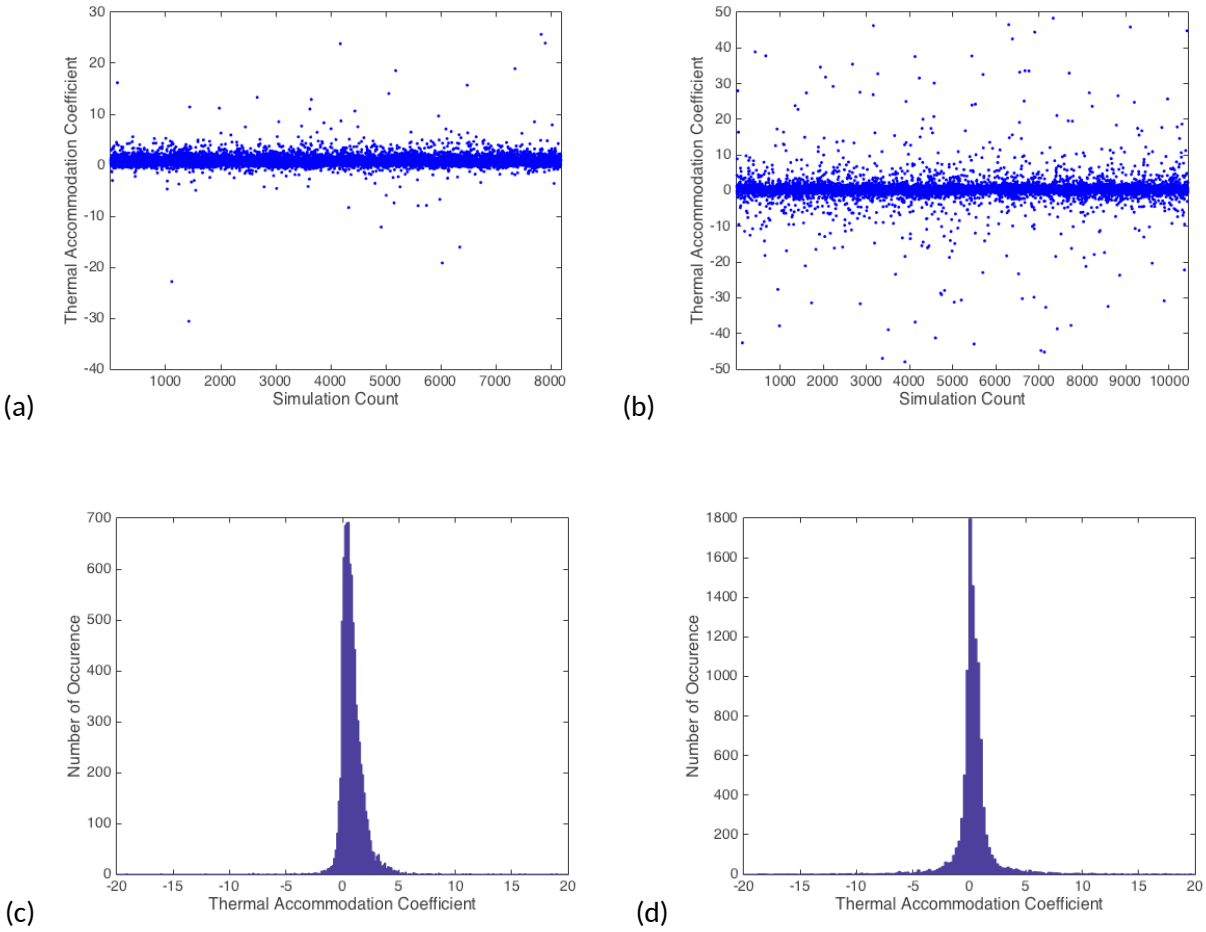

FIG. 5. Thermal accommodation coefficient distribution: (a) Ar – Al TAC vs simulation count scatterplot; (b) He – Al TAC vs simulation count scatterplot; (c) Ar – Al TAC histogram; (d) He – Al TAC histogram

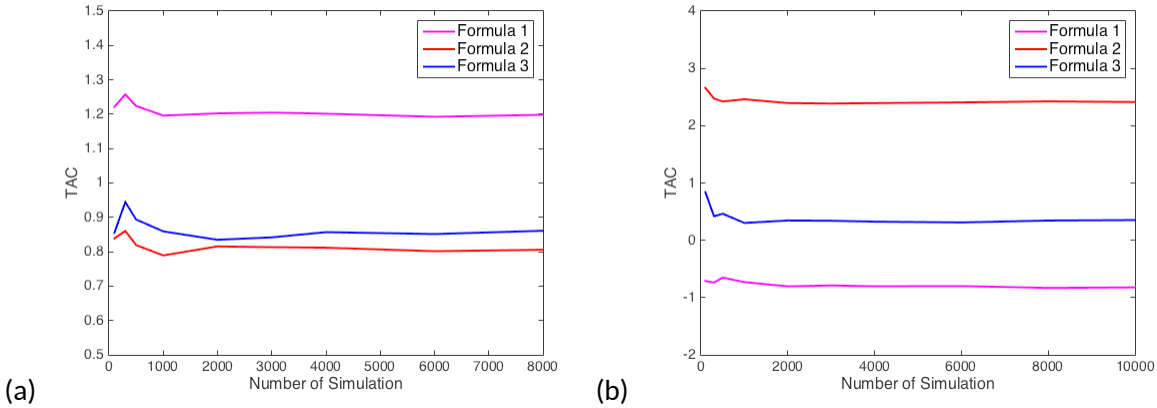

FIG. 6. Convergence of TAC with the number of individual simulation: (a) Ar – Al; (b) He – Al

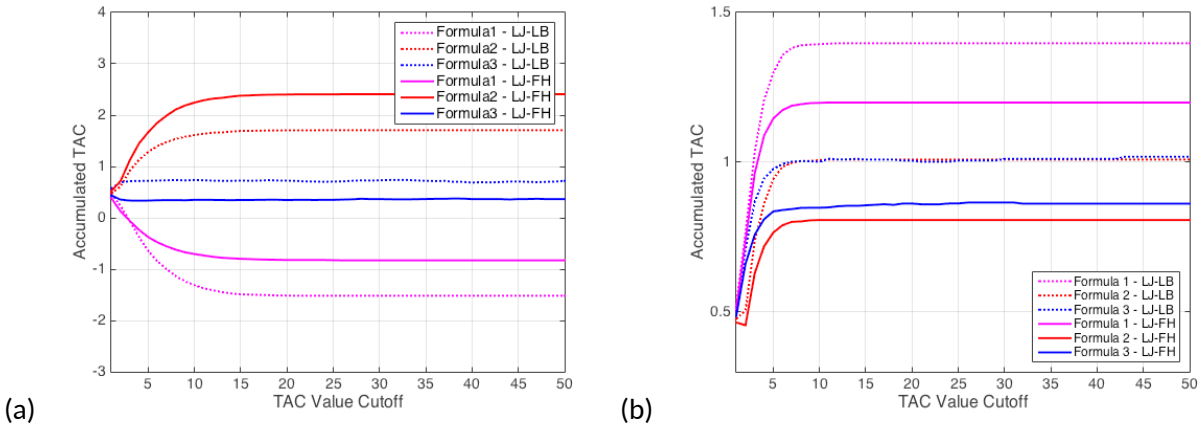

FIG. 7. Accumulated TAC varies with the selected TAC range: (a) He – Al, (b) Ar – Al

TABLE I. Noble gases – aluminum interatomic potential parameters

Potential	Atom Type	Parameters	
		ε / k_B (K)	σ (Å)
Lennard - Jones	Al [26]	4551.0	2.62
	He [27]	10.2	2.56
	Ar [27]	120.0	3.40

TABLE II. Thermal accommodation coefficients of helium and argon interacting with aluminum

	Thermal Accommodation Coefficient			
Atom pair	He – Al		Ar - Al	
Combining rules	Lorentz – Berthelot	Fender – Halsey	Lorentz - Berthelot	Fender – Halsey
Simulation Count	7745	10440	5646	8184
Formula 1	-1.5189 ± 0.0319	-0.8284 ± 0.0214	1.3974 ± 0.0180	1.1993 ± 0.0132
Formula 2	1.7078 ± 0.0240	2.4074 ± 0.0242	1.0088 ± 0.0174	0.8070 ± 0.0128
Formula 3	0.7195 ± 0.0491	0.3653 ± 0.0341	1.0182 ± 0.0201	0.8614 ± 0.0146
Exp Ref 1 [28]	0.38 (plasma treated), 0.47 (machined)		0.86	
Exp Ref 2 [29]	0.38 (plasma treated), 0.47(machined)		0.91 -0.96	
Exp Ref 3 [30]	0.53		0.81	